# Storage Compartments for Capillary Water Rarely Refill in an Intact Woody Plant[1][OPEN]

**Thorsten Knipfer,[a,2] Italo F. Cuneo,[b] J. Mason Earles,[a,c] Clarissa Reyes,[a] Craig R. Brodersen,[c] and Andrew J. McElrone[a,d,2]**

[a]Department of Viticulture and Enology, University of California, Davis, California 95616
[b]School of Agronomy, Pontificia Universidad Católica de Valparaíso, Quillota, Chile
[c]School of Forestry and Environmental Studies, Yale University, New Haven, Connecticut 06511
[d]U.S. Department of Agriculture-Agricultural Research Service, Crops Pathology and Genetics Research Unit, Davis, California 95618

Water storage is thought to play an integral role in the maintenance of whole-plant water balance. The contribution of both living and dead cells to water storage can be derived from rehydration and water-release curves on excised plant material, but the underlying tissue-specific emptying/refilling dynamics remain unclear. Here, we used x-ray computed microtomography to characterize the refilling of xylem fibers, pith cells, and vessels under both excised and in vivo conditions in *Laurus nobilis*. In excised stems supplied with water, water uptake exhibited a biphasic response curve, and x-ray computed microtomography images showed that high water storage capacitance was associated with fiber and pith refilling as driven by capillary forces: fibers refilled more rapidly than pith cells, while vessel refilling was minimal. In excised stems that were sealed, fiber and pith refilling was associated with vessel emptying, indicating a link between tissue connectivity and water storage. In contrast, refilling of fibers, pith cells, and vessels was negligible in intact saplings over two time scales, 24 h and 3 weeks. However, those compartments did refill slowly when the shoot was covered to prevent transpiration. Collectively, our data (1) provide direct evidence that storage compartments for capillary water refill in excised stems but rarely under in vivo conditions, (2) highlight that estimates of capacitance from excised samples should be interpreted with caution, as certain storage compartments may not be utilized in the intact plant, and (3) question the paradigm that fibers play a substantial role in daily discharge/recharge of stem capacitance in an intact tree.

Stem internal water storage can prolong vessel functionality by sourcing water into the transpiration stream and reducing the risk of gas emboli by buffering xylem tension (Tyree and Sperry, 1989; Holbrook, and Sinclair, 1992; Holbrook, 1995; Cochard et al., 2013). Estimates of water storage are commonly derived from water-release curves measured on excised stems (Tyree and Yang, 1990; Jupa et al., 2016). These data indicate that water stored in dead fibers, nonfunctional vessels, and apoplastic pores provide the largest fraction of stored water in most trees (i.e. capillary water storage). Living cells (e.g. xylem parenchyma) typically provide a relatively small storage volume due to their limited ability to expand, and this water is released under more negative xylem pressures (i.e. elastic water storage). Experiments by Borchert and Pockman (2005) indicate that storage compartments for capillary and elastic water refill during stem rehydration, and refilling of capillary water storage requires xylem pressures of greater than −0.5 MPa. However, the hydraulic methods used to measure elastic and capillary water storage require excised plant material released from sustained negative pressures, and the resulting data do not provide information about the temporal, spatial, or tissue-specific emptying or refilling dynamics of an intact plant.

Measurements on forest trees using sap flow sensors, isotopic tracers, frequency domain reflectometry, and dendrometers indicate that the emptying and refilling of storage compartments occurs on a daily basis (Goldstein et al., 1998; Cermák et al., 2007; Meinzer et al., 2009; De Schepper et al., 2012; Hao et al., 2013; Oliva Carrasco et al., 2015). In some species, a release of

[1] This work was supported by a USDA National Institute of Food and Agriculture SCRI grant and funding from the American Vineyard Foundation to A.J.M. and USDA-ARS CRIS funding (grant no. 5306-21220-004-00). The Advanced Light Source is supported by the Director, Office of Science, Office of Basic Energy Science, of the U.S. Department of Energy under contract no. DE-AC02-05CH11231.

[2] Address correspondence to tmknipfer@ucdavis.edu or ajmcelrone@ucdavis.edu.

The author responsible for distribution of materials integral to the findings presented in this article in accordance with the policy described in the Instructions for Authors (www.plantphysiol.org) is: Andrew J. McElrone (ajmcelrone@ucdavis.edu).

T.K. designed and performed most of the experiments, analyzed the data, and wrote the article together with A.J.M.; I.F.C., J.M.E., and C.R. performed some of the experiments, helped in data analysis, and revised the article; C.R.B. helped in experimental design, performed the ESEM imaging, and revised the article; A.J.M. obtained the grants, helped in experimental design, performed some of the experiments, and wrote the article together with T.K.

[OPEN] Articles can be viewed without a subscription.

www.plantphysiol.org/cgi/doi/10.1104/pp.17.01133

stored water from the trunk can contribute up to 50% to daily transpiration (Waring et al., 1979; Verbeeck et al., 2007), and tree transpiration can be maintained with stored water for about 1 week (Cermák et al., 2007). Current data suggest that the volume of stored and discharged water can be substantial, which implies that tissue compartments of relatively high storage capacity (such as dead fibers for storage of capillary water) are involved in this process and are able to refill on a regular (daily) basis. Similar to capillary water storage (Borchert and Pockman, 2005), successful vessel refilling appears to require xylem pressures approaching or exceeding 0 MPa (Hacke and Sperry, 2003; Charrier et al., 2016). Therefore, both refilling processes may be interrelated, and vessel refilling in some species may be limited by a simultaneous recharge of capacitive tissue and competition for free water. The link among refilling of water storage compartments and vessel refilling remains to be determined.

A large body of literature has been published over the last few decades concerning the importance of plant water storage (examples cited above). Here, our goal was to visualize the refilling dynamics of the putative compartments for water storage (fibers and pith) and long-distance, axial transport (vessels) under both excised and in vivo conditions, and to determine whether the laboratory-based hydraulics methods used to study capacitance are measuring the same processes that occur in an intact plant. In turn, these data would then provide novel insight into the role of different tissue types in plant hydraulic function. Experiments using noninvasive high-resolution x-ray computed microtomography (microCT) imaging were complemented with traditional microscopy and physiological measurements. Our study was performed on *Laurus nobilis*, an evergreen woody plant native to the Mediterranean region that has been documented for its ability to restore plant hydraulic function by vessel refilling (Salleo et al., 1996; Hacke and Sperry, 2003; Trifilò et al., 2014).

## RESULTS

### Excised Stem

During the rehydration of excised *L. nobilis* stems, water uptake revealed two distinct phases over a period of 20 h (Fig. 1A). The initial phase of uptake was rapid (less than 1 h), followed by a second phase that was relatively slow but steady. A biphasic response in water uptake was observed in stems both with and without leaves, indicating that this response predominantly reflected stem internal water storage dynamics. During the initial uptake phase, $\Psi_{stem}$ recovered to values close to 0, and $\Psi_{stem}$ stabilized during the second phase. The biphasic response curve indicated that different tissue compartments refilled during the rehydration process (Fig. 1A), and the relationship of $\Psi_{stem}$ and water uptake pointed to differences in hydraulic capacitance among these compartments (Fig. 1B). The capacitance of tissue compartments providing for initial water storage was low (0.02–0.06 g $MPa^{-1}$), whereas the capacitance of compartments providing for storage after more than 1 h of rehydration was much greater (1.7–11.9 g $MPa^{-1}$) (Fig. 1B).

Tissue-specific refilling during the rehydration of excised stems was visualized using microCT imaging. For a representative excised stem supplied with water (Fig. 2), fibers located in older xylem close to pith and many fibers throughout the second annual ring were initially air filled ($A_{air\text{-}fibers}$ = 0.09 $mm^2$; Fig. 2A; $t$ = 2.5 h). At the same time, many pith cells were air filled ($A_{air\text{-}pith}$ = 0.4 $mm^2$), and the majority of embolized vessels were located in older xylem close to pith ($A_{air\text{-}vessels}$ = 0.04 $mm^2$; Fig. 2A; $t$ = 2.5 h). A few hours later, during stem rehydration, $A_{air\text{-}fibers}$ (0.05 $mm^2$) was reduced by 45% and $A_{air\text{-}pith}$ (0.33 $mm^2$) was reduced by 18%; simultaneously, more embolized vessels appeared ($A_{air\text{-}vessels}$ = 0.05 $mm^2$; Fig. 2A; $t$ = 7.5 h). After 14 h, $A_{air\text{-}fibers}$ was as low as 0.01 $mm^2$ (Fig. 2A). After 18.5 h, very few air-filled fibers remained in the most recent annual ring, while all fibers in older xylem close to pith had refilled ($A_{air\text{-}fibers}$ = 0.003 $mm^2$; Fig. 2A). Remaining air-filled pith cells were concentrated toward the stem center ($A_{air\text{-}pith}$ = 0.16 $mm^2$), and many air-filled vessels persisted in an embolized state (Fig. 2A; $t$ = 18.5 h). These refilling dynamics were confirmed with 3D observations during a 6.5-h period (Fig. 2B); as visualized for a portion of the stem, the air-filled volume of fibers and pith decreased from 0.006 to 0.003 $mm^3$ and from 0.135 to 0.055 $mm^3$, respectively, while changes in air-filled vessel volume were negligible.

Across all excised stem samples, temporal dynamics of refilling differed among tissue compartments and among treatments when stems were either rehydrated (Fig. 3, A–C) or entirely sealed (Fig. 3, D–F; for cross-sectional areas, see Supplemental Table S1). In excised stems during rehydration, $A_{air\text{-}fibers}$ declined rapidly (Fig. 3A), while $A_{air\text{-}pith}$ declined at a slower pace compared with fibers (Fig. 3B). Simultaneously, $A_{air\text{-}vessels}$ typically increased in the first couple of hours and decreased thereafter (Fig. 3C). Curves fit to the data using nonlinear regressions indicated that 50% of air-filled fibers refilled within around 5 h of rehydration (Fig. 3A); in comparison, a 50% reduction in air-filled pith tissue and vessels typically required more than 15 and 35 h, respectively (Fig. 3, B and C). Refilling of air-filled fibers and pith tissue also was observed for stems that were entirely sealed (Fig. 3, D and E), but $A_{air\text{-}fibers}$ and $A_{air\text{-}pith}$ declined more slowly as compared with rehydrated stems; curves fit to the data using nonlinear regressions indicated a 50% reduction of $A_{air\text{-}fibers}$ and $A_{air\text{-}pith}$ after around 30 h. Moreover, refilling of fibers and pith tissue was accompanied by a general increase in embolized vessels (Fig. 3F), pointing to internal water redistribution from vessels to refilling fibers and pith (see circle symbols); increases in embolized vessels were least pronounced for the sample indicated with diamond symbols (Fig. 3F), which suggests that water

from alternative tissue sources also was redistributed toward fiber and pith.

MicroCT images provided visual evidence that tissue-specific refilling in stems was dominated by capillary forces (Fig. 4), and as shown for a representative excised stem during rehydration, transverse images showed that the lumen of several adjacent air-filled fibers appeared water filled 3 h later (Fig. 4A). Corresponding longitudinal images indicated that, while fibers refilled, water columns expanded inside the air-filled lumen from both ends (Fig. 4, B and C), and the liquid/air meniscus with the fiber wall was concave shaped relative to the direction of flow (the contact angle ranged from 44° to 63°; for fibers located close to and farther away from pith, see Supplemental Fig. S1). For pith tissue (Fig. 4, D and E), enlarged longitudinal images showed that air-filled cells located in proximity to xylem refilled first (Fig. 4D). Refilling and water entry into the air-filled pith cell initially resulted in the formation of a concave-shaped liquid/air meniscus with the cell wall and the appearance of a spherical air void before the completion of refilling (Fig. 4E). Refilling of the air-filled vessel lumen was related to water droplet formations on the lateral vessel wall and water column expansion (Fig. 4F); the liquid/air meniscus with the vessel wall was variable in shape.

### Intact Plant

In contrast to excised conditions, tissue-specific refilling was negligible in the stem of intact saplings (Figs. 5 and 6). In a representative *L. nobilis* sapling, $\Psi_{stem}$ recovered from −1.5 to −0.4 MPa after 20 h of soil rehydration, but $A_{air\text{-}fibers}$ (0.58 $mm^2$), $A_{air\text{-}vessels}$ (0.17 $mm^2$), and $A_{air\text{-}pith}$ (0.54 $mm^2$) remained at similar levels under in vivo conditions (less than 6% change; Fig. 5, A and B). In line with previous observations, after the stem was excised and rehydrated for 5.5 h, $A_{air\text{-}fibers}$ declined by 43% to 0.33 $mm^2$, which was accompanied by 13% and 23% reductions of $A_{air\text{-}pith}$ and $A_{air\text{-}vessels}$, respectively.

For intact saplings with the shoot not bagged and exposed to ambient conditions (Fig. 6, A–C), changes in $A_{air\text{-}fibers}$, $A_{air\text{-}pith}$, and $A_{air\text{-}vessels}$ by refilling were minimal during recovery in $\Psi_{stem}$ (from less than −1 to ~−0.5 MPa following soil saturation after drought). Similarly, in intact saplings that were maintained well watered and that entered the experiment at less negative $\Psi_{stem}$ (−0.5 and −0.4 MPa), no continuous reductions in $A_{air\text{-}fibers}$, $A_{air\text{-}pith}$, and $A_{air\text{-}vessels}$ were observed, even after maintaining saplings under well-watered conditions for an additional 3 weeks (Fig. 6). However, for well-watered saplings where the shoot was bagged during the time period of investigation, there was evidence of slow but gradual reductions in $A_{air\text{-}fibers}$, $A_{air\text{-}pith}$, and $A_{air\text{-}vessels}$ over time (Fig. 6, D–F); curves fit to the data using nonlinear regressions indicated that refilling of tissues for the bagged plants resulted in reductions of $A_{air\text{-}fibers}$, $A_{air\text{-}pith}$, and $A_{air\text{-}vessels}$ by around 20% after 20 h.

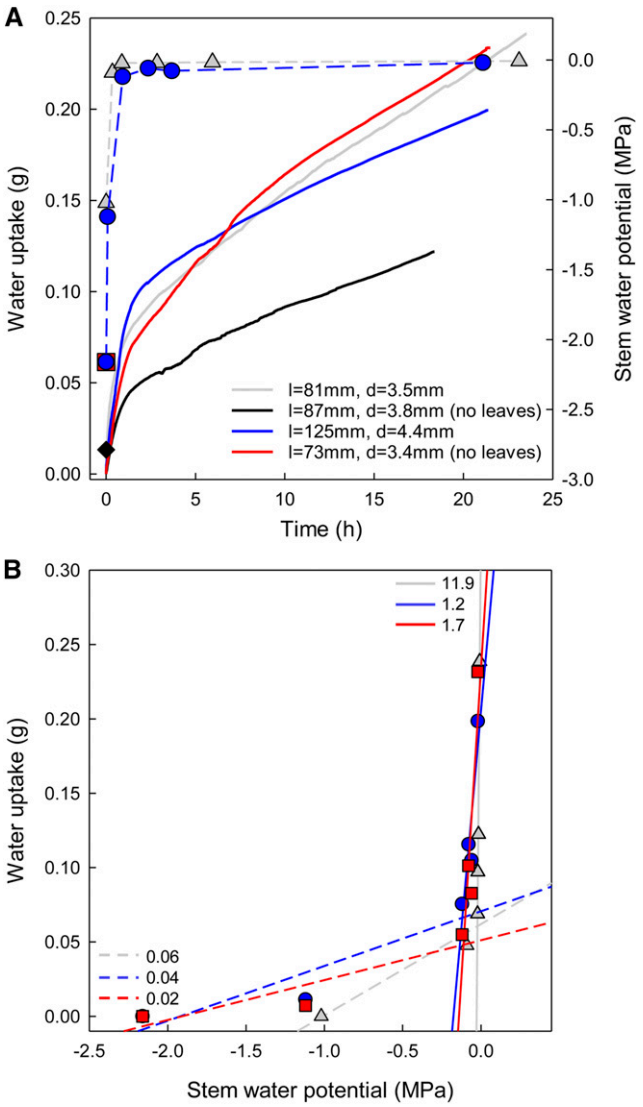


**Figure 1.** A, Time course of water uptake (indicated by solid lines) and corresponding stem water potential ($\Psi_{stem}$; indicated by symbols) during rehydration of excised *L. nobilis* stems. Following the measurement of initial $\Psi_{stem}$ (time = 0 h), the stem was connected to a water source and the stem surface and leaves were sealed to prevent evaporation during rehydration. Values in the legend are lengths and diameters of excised stems. Stems indicated in blue (with leaves to measure $\Psi_{stem}$) and red (no leaves) were obtained from the same branch and analyzed simultaneously. B, Relationship of $\Psi_{stem}$ and the corresponding amount of water uptake. For analysis of the stem indicated in red (no leaves), $\Psi_{stem}$ values of the stem indicated in blue were used. Linear regression analysis was performed to determine the capacitance (values in g $MPa^{-1}$) of elastic (dashed line fitted across data points 1 to 3 at most negative $\Psi_{stem}$) and capillary (solid line fitted across data points 3 to 6) storage compartments.

### Stem Anatomical Features

Tissue viability staining showed that fibers in stem xylem were not metabolically active and were dead, as were most pith cells toward the stem center (Fig. 7, A–C). Xylem parenchyma cells were relatively inactive

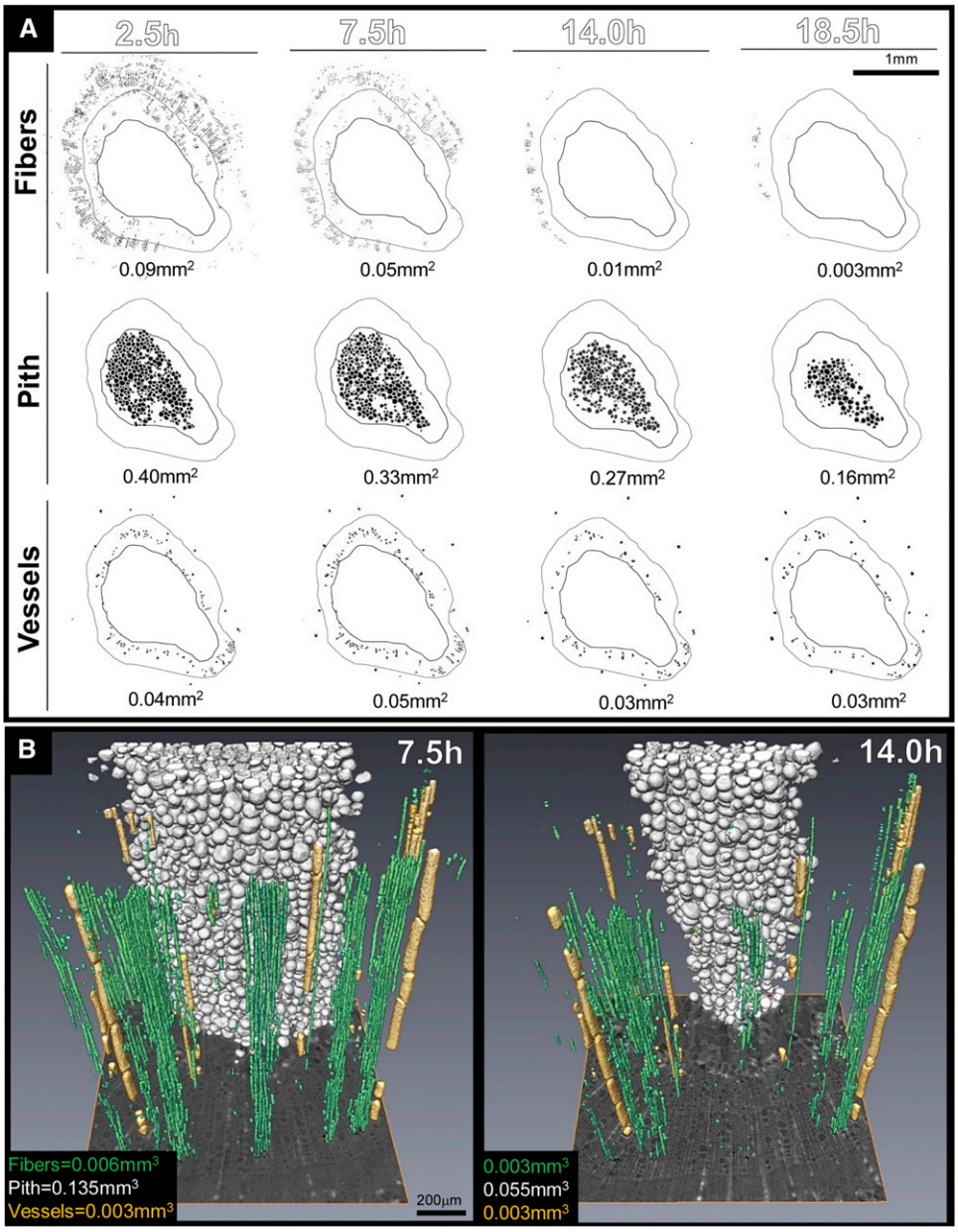


**Figure 2.** Visualization of tissue-specific refilling dynamics during rehydration (at $t = 0$ h) of an excised *L. nobilis* stem (length of ~5 cm containing no leaves; indicated by circle symbols in Fig. 3, A–C). A, Binary images were generated from transverse microCT images and show air-filled fibers (top row), pith tissue (middle row), and vessels (bottom row) in black. Values in $mm^2$ are air-filled cross-sectional areas; lines indicate the estimated boundaries between xylem annual rings (dashed lines) and xylem to pith (solid thick lines). B, Corresponding 3D visualizations of air-filled fibers (green), pith tissue (white), and vessels (gold) for a portion of the stem. Values in $mm^3$ are air volumes (some of the air-filled protoxylem vessels were excluded to allow for a better view of pith).

in their metabolic activity at the time of analysis, as is evident from small amounts of ray tissue emitting a green fluorescence signal. Within the pith, only cells located closest to xylem tissue (the first one to three cell layers) were living (Fig. 7, A–C). Anatomical features of fibers, pith tissue, and vessels were further characterized using environmental scanning electron microscopy (ESEM) and microCT imaging (Fig. 7, D–F). ESEM images showed the existence of fiber-to-fiber pits (Fig. 7D) and vessel-to-vessel bordered pits (Fig. 7E). MicroCT images showed that fibers were arranged in parallel rows and adjacent fibers were interconnected via pits (Fig. 7F); the lumen of fibers reconstructed in 3D (in red color) was clearly visible through pit openings after fibers were sliced open (Fig. 7F, image 1). Images from 3D volume renderings also indicated that fibers were connected to neighboring vessels (predominantly in a tangential direction). 3D volume renderings of the pith showed that the cell wall contained many cell-to-cell connections (Fig. 7F, image 2).

## DISCUSSION

Water storage and release has been described as an integral physiological process that contributes to whole-plant water balance (Tyree and Sperry, 1989; Holbrook, 1995; Hao et al., 2013). In this study on

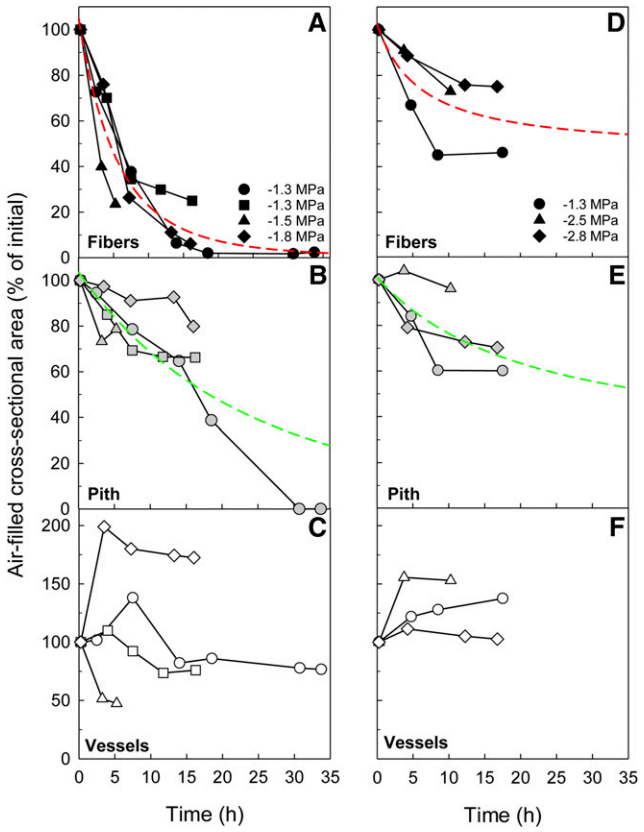


**Figure 3.** Temporal refilling dynamics of air-filled fibers, pith tissue, and vessels in excised *L. nobilis* stems that were either supplied with water at cut ends (A–C) or sealed entirely (D–F). Values in MPa are initial $\Psi_{stem}$ measured prior to sample preparation; all excised stems contained no leaves. Dashed lines provide an estimate of tissue-specific refilling dynamics and were obtained from nonlinear regression analysis across data points of all samples ($y = a \times e^{(b/(x+c))}$; A, a = 0.004, b = 582, c = 57, $R^2 = 0.92$, $P < 0.0001$; B, a = 0.005, b = 2279, c = 229, $R^2 = 0.73$, $P < 0.0001$; D, a = 46, b = 7, c = 8, $R^2 = 0.63$, $P = 0.018$; E, a = 25, b = 56, c = 40, $R^2 = 0.60$, $P = 0.02$; lines were omitted for C and F, where a continuous trend of refilling was lacking).

*L. nobilis*, we characterized the tissue-specific refilling dynamics related to capillary water storage under both excised and intact (in vivo) conditions, which revealed significant differences between rehydration processes that take place within the stem of an intact plant compared with those that occur in the type of excised stem material generally used for hydraulics measurements in the laboratory. Time-series microCT imaging indicated that, in intact saplings, refilling of fiber and pith tissue was negligible over periods ranging from 20 h to 3 weeks unless the shoot of the sapling was bagged and completely covered with petroleum jelly to prevent any cuticular water loss and transpiration. In comparison, fiber and pith tissue refilled within hours in excised stems during rehydration. It can be speculated that *L. nobilis*, which is a Mediterranean species, would only experience these conditions infrequently during the growing season, if at all, or during rainy winter months that coincide with soil saturation, lower transpiration, and a wet canopy (LoGullo and Salleo, 1988; Rhizopoulou and Mitrakos, 1990). Contrary to the diurnal discharge and refilling of water from living cells in the bark (De Schepper et al., 2012), our data indicate that, for small trees, (1) refilling of dead tissue compartments with capillary water is an exception and not the rule under in vivo and transpiring conditions, and (2) dead fiber and pith tissue plays a negligible role in buffering the daily fluctuation in xylem tensions in an intact tree once empty (i.e. single-use water reservoir). Our conclusions are based on the dynamics of refilling from the saplings studied here, but they need to be tested to determine if these results extend to larger trees in the field, across species that differ in stem anatomical features and those that grow in different climate regions.

Several research groups have documented large daily cycles of capacitance discharge and subsequent recharge in trunks of large trees (Goldstein et al., 1998; James et al., 2003; Cermák et al., 2007; Hao et al., 2013). These authors concluded that (1) water storage is important for maintaining short- and long-term plant water balance (Hao et al., 2013); (2) the diurnal withdrawal of water from, and refill of, internal stores is a dynamic process (Goldstein et al., 1998); (3) the exchange of water between storage compartments and the transpiration stream has a substantial influence on axial and radial stem water transport (James et al., 2003); and (4) sapwood is the most important storage site for water (Cermák et al., 2007). Our study was performed on young intact saplings, and while we cannot comment directly on the contribution of the trunk of large trees to water storage, we have, to our knowledge for the first time, pinpointed the exact sites of capillary water storage while also characterizing the limitations to their refilling.

Since the process of capillary water storage in plants should follow the same biophysical rules independent of stem age, size, or organ type (for fiber refilling, see discussion below), our data raise some valid concerns about the current paradigm that capillary water storage (such as in dead fibers) contributes to the daily discharge and recharge of stem capacitance. If this phenomenon extends beyond *L. nobilis* and is present in other tree species and mature trees, this would require a significant revision of our understanding of xylem function. However, many open questions still remain. Which capacitive tissue compartments provide a means to protect xylem function under drought? How is water redistributed within stems to buffer daily fluctuations in xylem sap tension? Are there fiber types with specialized anatomical structures that facilitate water storage and release in certain plant species?

Our current knowledge of tissue-specific water storage is largely based on measurements of water-release and rehydration curves obtained from excised material (Tyree and Yang, 1990; Borchert and Pockman, 2005;

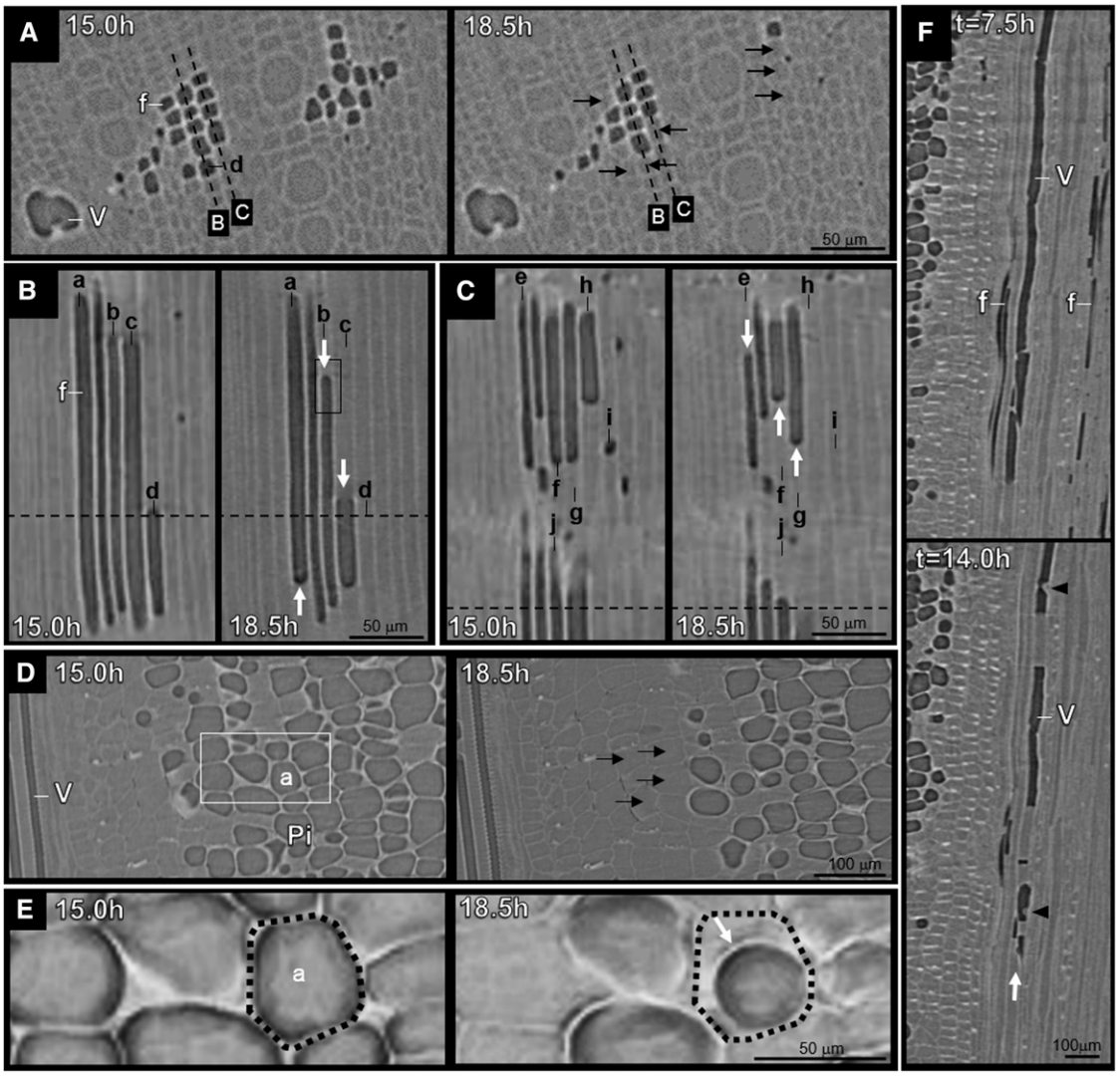


**Figure 4.** Visualization of the refilling process of air-filled fibers (A–C), pith (D and E), and vessels (F) in an excised *L. nobilis* stem during rehydration (at $t = 0$ h; circle symbols in Fig. 3, A–C). Representative microCT images show water- and air-filled tissue in light and dark gray, respectively. A, Enlarged transverse images show adjacent air-filled fibers, and many of these fibers refilled over time (examples indicated by black arrows). B and C, Corresponding longitudinal images show the expansion of water columns (the direction of movement is indicated by white arrows) inside the air-filled lumen; fibers labeled a to d and e to j were positioned along dashed lines B and C, respectively, in A. Liquid/air menisci with the fiber wall were concave shaped. D, Longitudinal images show the progression of pith refilling from the periphery toward the stem center (black arrows indicate examples of refilled cells). E, Corresponding 3D volume rendering for an enlarged portion of the pith (position indicated by the white box in D) visualizing cell a during refilling (the dashed line indicates the cell wall). The liquid/air meniscus with the cell wall was concave shaped. F, Longitudinal images show refilling of an air-filled vessel. Water columns formed and expanded inside the air-filled lumen (the direction of movement is indicated by white arrows); black triangles indicate droplets forming on the lateral vessel wall (f, fiber; Pi, pith; V, vessels).

Oliva Carrasco et al., 2015; Jupa et al., 2016). The advantage of using hydraulic methods is that it allows the researcher to obtain the exact volume of water released/stored for a given change in water potential; in turn, the capacitance of different tissue compartments (capillary versus elastic storage) can be derived from the shape of the curve. Water-release curves provide data for tissue-specific capacitance, but direct observations of tissue-specific water storage are lacking for most woody species under in vivo conditions. Using microCT imaging, we were not able to determine capacitance and volume fractions of water in different tissue regions, but we were able to visualize that substantial temporal differences in fiber refilling can exist under in vivo and excised conditions, potentially complicating the interpretation of measurements on

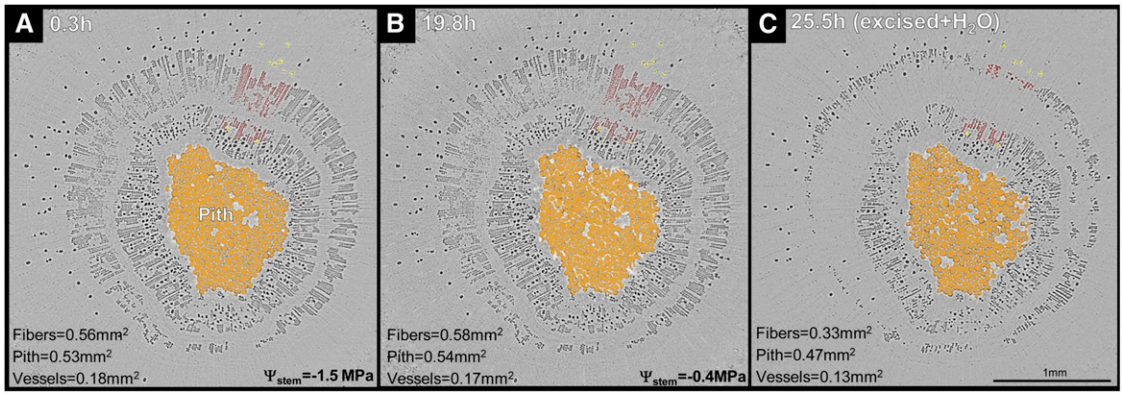


**Figure 5.** Transverse microCT images visualizing air-filled tissues in the stem of an intact *L. nobilis* sapling following soil saturation (at $t = 0$ h; A and B) and following stem excision (length ~ 5 cm) and rehydration for 5.5 h (C). For better orientation, examples of the same air-filled fibers and vessels are labeled in red and yellow, respectively, and air-filled pith tissue is labeled in orange. Values in h represent time following soil saturation; values in $mm^2$ represent air-filled cross-sectional areas.

excised material. For intact *L. nobilis* saplings, our microCT data show that fibers rarely refill in vivo after soil saturation, suggesting that estimates of capillary water storage obtained on excised woody stems should not be considered as a significant part of the overall stem water storage capacity once these compartments have emptied in the intact plant; otherwise, this may overestimate the real water storage capacity that the intact plant utilizes on a regular basis. Nevertheless, the exact implications of our findings for intact, mature trees in the field need to be investigated in more detail in future experiments.

Woody tree species growing in dry environments typically experience low $\Psi_{stem}$ values of less than −1.5 MPa throughout the year, and species with a high abundance of nonliving tissue and denser wood usually exhibit the most negative $\Psi_{stem}$ (Borchert and Pockman, 2005; Meinzer et al., 2009). In *L. nobilis*, $\Psi$ ranges from −0.4 to −2.5 MPa over the growing season, reaching most negative values in late summer (LoGullo and Salleo, 1988; Nardini et al., 1996). Nardini et al. (2017) showed that water is lost from fibers under water stress in *L. nobilis*, but this observation was not addressed in detail, and fiber refilling was not investigated. For *L. nobilis* and other tree species, this raises the question of how and if compartments for capillary water storage refill. To date, microCT imaging data by Suuronen et al. (2013) provide the only visual evidence for refilling of fibers, which was dependent on environmental conditions such as high temperatures and darkness. Similarly, our data highlight that both fiber and pith refilling requires environmental conditions that, presumably, induce a substantial relaxation of xylem tension. The data collected here during rehydration of excised stems indicated that capillary water storage in dead fibers and pith requires a local $\Psi_{stem}$ of greater than −0.1 MPa in *L. nobilis*.

Water transport from vessels into the fiber lumen and among fibers is generally considered to occur via pits (Siau, 1984). In Lauraceae species, xylem fibers are typically of the libriform type, dead, with thick walls, and simple bordered pits (Esau, 1953; Schweingruber et al., 2011). Similarly, the fibers studied here were nonseptate with scanty pitting to adjacent vessels or fibers. MicroCT data obtained from excised stems that were entirely sealed (no water supplied) showed that additional vessels embolized while fibers refilled simultaneously, pointing to water transport via pits during this process. Tyree et al. (1999) showed that vessels in *L. nobilis* are surrounded in places by paratracheal parenchyma cells that separate the vessel lumen from fibers. Because xylem cavitation in *L. nobilis* is thought to be nucleated by microbubbles entering the vessel lumen (Salleo et al., 1996), and fibers can function like transport bridges among vessels (Cai et al., 2014), it can be speculated that this layer of paratracheal parenchyma may impose an important barrier restricting the passage of air from fibers toward remaining functional vessels.

Tradeoffs between xylem efficiency and embolism safety have been linked to water storage and fiber traits in angiosperms (for review, see Pratt and Jacobsen, 2017). For *L. nobilis* saplings as used here, microCT data combined with additional transpiration measurements indicated that water lost from fibers would only contribute a negligible amount of water to the transpiration stream. Calculations showed that a volume of water equivalent to the maximum volume of air-filled fibers in the stem (approximated to be on average 6% = $A_{air\text{-}fibers}/A_{stem}$; Supplemental Table S1) would be transpired in only 2 min during the daytime (transpiration rate of $4 \pm 0.4 \times 10^{-6}$ $m^3$ $h^{-1}$, measured gravimetrically from the water loss of potted saplings where the soil was covered with plastic foil) and 30 min during the nighttime

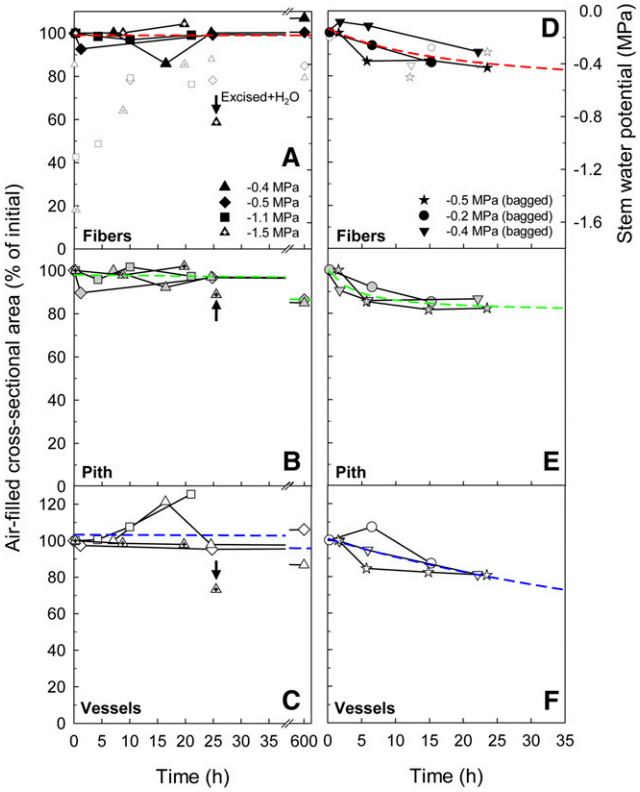


**Figure 6.** Temporal refilling dynamics of air-filled fibers, pith tissue, and vessels in the stem of intact *L. nobilis* saplings. During the time period of investigation, the soil was fully saturated for all saplings. The shoot of saplings was either exposed to ambient conditions (A–C) or covered in petroleum jelly and a humid plastic bag (D–F). $\Psi_{stem}$ (white symbols in A and D) of saplings was monitored periodically; values in legend are initial $\Psi_{stem}$ of saplings. As for Figure 3, dashed lines provide an estimate of tissue-specific refilling dynamics and were obtained from nonlinear regression analysis across data points of all samples ($y = a \times e^{(b/(x+c))}$; A, a = 98, b = 4E-11, c = 1, $R^2 = -1.64E\text{-}11$, $P = 1$; B, a = 47, b = 2156, c = 2953, $R^2 = 0.58$, $P = 0.005$; C, a = 0.73, b = 1002, c = 201, $R^2 = 0.63$, $P = 0.01$; D, a = 72, b = 8, c = 24, $R^2 = 0.63$, $P = 0.02$; E, a = 80, b = 1, c = 5, $R^2 = 0.8$, $P = 0.001$; F, a = 12, b = 421, c = 195, $R^2 = 0.66$, $P = 0.01$).

($0.3 \pm 0.01 \times 10^{-6}$ m$^3$ h$^{-1}$); for calculations, the estimated stem volume and maximum air-filled fiber volume of saplings (leaf area was 25,693 ± 1,211 mm$^2$) were 2,596 ± 73 mm$^3$ (as derived from stem height and diameter) and 159 ± 4 mm$^3$, respectively. Since the amount of water released from fibers was relatively small compared with the volume of water transpired and fibers rarely refilled in vivo, it can be inferred that fibers are rather ineffective in discharging water into the transpiration stream to buffer daily fluctuations in xylem tensions in *L. nobilis* saplings. However, water stored in fibers may have been large enough to be of relevance on a localized tissue level by providing water to xylem parenchyma cells, thereby allowing for turgor maintenance and cell function when xylem tensions fluctuated, but this topic needs more in-depth experimental testing.

In theory, fibers can only rehydrate if the liquid/air meniscus inside the lumen is able to overcome the negative pressure in neighboring xylem vessels ($P_x$). The negative pressure ($P$, relative to atmospheric pressure) of a water column inside a cylindrical tube can be estimated according to the Young-Laplace equation:

$$P = 2\gamma\cos(\Theta)/r$$

where $\gamma$ is the surface tension of water (0.072 N m$^{-1}$), $\Theta$ is the liquid/wall contact angle of the meniscus, and $r$ is the radius. MicroCT images collected in this study showed that fibers had a radius ranging from 2.5 to 9 $\mu$m. For a concave-shaped meniscus with a contact angle of around 60°, we estimated a $P$ of −0.001 to −0.005 MPa, which suggests that only under conditions where $P_x$ is greater than −0.005 MPa will water enter the air-filled lumen via capillary forces. Given that vessels and pith cells were of larger lumen diameter than fibers, it would require $P_x >> -0.005$ MPa for those compartments to refill solely by capillarity. Such values were not obtained from indirect measurements of xylem pressure by $\Psi_{stem}$, but it can be speculated that such pressures exist locally where refilling of these tissue compartments was observed.

Pith tissue commonly suffers mechanical damage during development, and cells lose their ability to store carbohydrates and become devoid of content as stems mature (Esau, 1953). Under drought and stem elongation, autolysis of pith cells is a common phenomenon leading to air-filled cell cavities (for review, see Beers, 1997). Together, microCT and fluorescent light microscopy images provided visual evidence for the spatial distribution of dead and living pith cells in young stems of *L. nobilis*, and the data indicate that most pith cells are air-filled, dead, and devoid of starch granules, while the remaining living pith cells are located at the periphery close to the xylem. Our data suggest that xylem parenchyma and pith cells close to xylem may have been the only effective site for carbohydrate storage (Plavcová and Jansen, 2015). Furthermore, in woody stems with extensive secondary growth, the pith tissue typically becomes crushed and disappears. Our microCT data on *L. nobilis* indicated that, before the pith becomes crushed, air-filled cavities of dead pith cells can fill with water, especially for excised samples. In turn, water released from dead pith cells may contribute significantly to the measured water volume obtained from water-release curves, especially when dead pith tissue occupies a large fraction of the entire organ volume.

Recent literature indicates that most woody plant species lack an efficient mechanism for short-term (days) embolism repair in vivo (Brodersen and McElrone, 2013; Cochard and Delzon, 2013; Choat et al., 2015 [redwood {*Sequoia sempervirens*}]; Knipfer et al.,

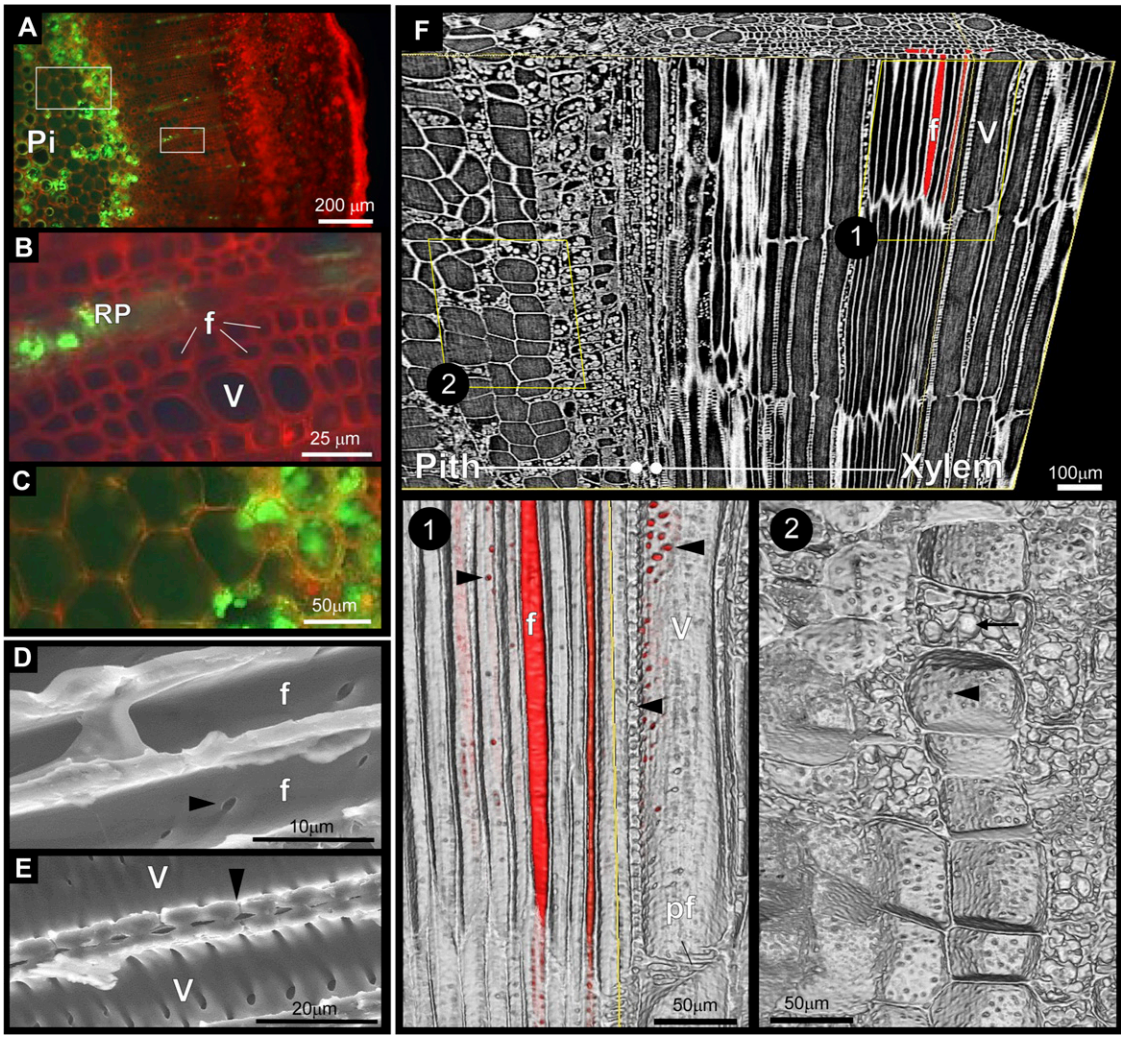


**Figure 7.** Characterization of tissue viability and anatomical features in *L. nobilis* stems. A to C, Fluorescence light microscopy images stained with fluorescein diacetate (FDA; green signal inside viable tissue) and propidium iodide (PI; red signal in nonviable apoplast) solutions. Corresponding enlarged images (locations indicated by the white boxes in A) show that fibers surrounding vessels were dead (B) and that only xylem ray parenchyma and pith cells located in close proximity to xylem were living (C); pith cells located farther inward were dead but maintained an intact cell wall. D and E, ESEM images show pit connections (indicated by arrowheads) between fibers and between vessels. F, MicroCT longitudinal images show that adjacent fibers were arranged in radial rows; examples of fiber lumen are reconstructed in 3D and labeled in red. Images 1 and 2 (positions indicated by the yellow boxes in F) show enlarged images of 3D volume renderings. Fiber-to-fiber, vessel-to-fiber, and vessel-to-vessel pits in xylem (image 1) and cell-to-cell connections in pith (image 2) are clearly visible; examples of pits and cell-to-cell connections are indicated by black arrowheads. Examples of granules in pith cells are indicated by the arrow (f, fiber; Pi, pith; RP, ray parenchyma; V, vessel).

2015a [walnut {*Juglans microcarpa*}]), with grapevine (*Vitis vinifera*) as the exception (Brodersen et al., 2010; Knipfer et al., 2015b, 2016; Charrier et al., 2016). However, CryoSEM data collected by Tyree et al. (1999) indicate that embolism repair in *L. nobilis* is associated with water droplets emerging from lateral walls similar to in vivo observations in grapevine (Brodersen et al., 2010; Knipfer et al., 2015b, 2016). In line with these findings, our microCT images emphasize that *L. nobilis* stems have the ability to form water droplets on lateral vessel walls and refill by water column expansion, but over the time course of investigation vessel refilling was insignificant. Hacke and Sperry (2003) reported that vessel refilling in *L. nobilis* required the maintenance of plants at $\Psi_{stem} > -0.3$ MPa for 1 h by pressurizing the root system. Together with our data, it can be followed that a mechanism for short-term embolism repair by water droplet growth is mostly inactive in *L. nobilis* and water column expansion inside the vessel lumen also may be related to capillary action, similar to the refilling mechanism of dead fibers and pith cells at $\Psi_{stem}$ values close to zero.

## MATERIALS AND METHODS

### Plant Material

Experiments were performed on excised stem material as obtained from terminal branches of *Laurus nobilis* trees growing at the Arboretum, University of California, Davis. Terminal branches were harvested with pruning shears about 1 m behind the shoot tip and maintained in a sealed plastic bag containing a moist paper towel prior to analysis. In addition, in vivo experiments were performed on the main stem of intact *L. nobilis* saplings (approximately 30 cm in height) that were obtained from ArtForm Nurseries. Saplings ($n = 7$ in total) were grown in 4-inch-diameter plastic pots filled with a soil mix (equals parts of peat moss, composted bark, sand, and perlite) and maintained for more than 4 weeks under greenhouse conditions (approximate day/night temperatures of 8°C/25°C, photoperiod of 15/9 h, and relative humidity of 35%) at the University of California, Davis. Saplings were irrigated daily with water supplemented with macronutrients and micronutrients (similar to Knipfer et al., 2015a, 2015b). Prior to analysis, some saplings were subjected to drought by not watering for 3 to 7 d, while others were maintained under well-watered conditions. Because we were not able to monitor the entire growth period of *L. nobilis* branches or saplings, the plant material used may have experienced some level of stress resulting in air embolism prior to investigation.

#### $\Psi_{stem}$

The water status of intact saplings and harvested branch material was measured with a Scholander Pressure Chamber (Plant Moisture Stress model 1505D; PMS Instrument) on mature leaves that were covered and sealed with a foiled plastic bag for more than 30 min (Knipfer et al., 2015a, 2015b). The measured parameter was defined as $\Psi_{stem}$.

### Water Uptake Curves

Terminal branches were harvested and transported to the laboratory as described above in "Plant Material." In the laboratory, the branches were maintained for 1 to 2 h in the sealed plastic bag to allow for $\Psi_{stem}$ equilibration. Subsequently, initial $\Psi_{stem}$ was measured on an apical and a basal leaf, which were located at opposite sides of the stem portion of interest (length of 7–13 cm containing six leaves). When corresponding $\Psi_{stem}$ values differed by less than 0.05 MPa, the stem surface and leaves were covered with petroleum jelly and plastic foil to prevent evaporation, and the portion of interest was excised with a fresh razor blade from the branch. The apical cut of the excised stem was sealed with petroleum jelly, and a 2-cm piece of PVC tubing was placed over this stem end to hold the petroleum jelly in place. The distal cut was connected to water-filled PVC tubing that was inserted into a water-filled cylinder that was sitting on an electronic balance (Mettler). Stem water uptake was recorded continuously in 30-s intervals by weight change of the cylinder. During stem rehydration, $\Psi_{stem}$ was measured on leaves harvested from the excised stem. Water uptake also was measured for excised stems, for which all leaves were removed during sample preparation and prior to analysis. Stem hydraulic capacitance was determined from the slope (in g $MPa^{-1}$) of the linear portions of the relationship of $\Psi_{stem}$ versus water uptake (Borchert and Pockman, 2005).

### X-Ray Microtomography

Plant material was scanned at the x-ray microtomography facility (Beamline 8.3.2) at the Lawrence Berkley National Laboratory. Saplings were transported by car to the Advanced Light Source (Lawrence Berkeley National Laboratory) less than 4 h prior to analysis. To assess the impact of initial plant water status on the tissue-specific dynamics of refilling, saplings subjected to microCT analysis covered a range of initial $\Psi_{stem}$ values (−1.5 to −0.2 MPa) as measured at the Advanced Light Source after arrival. During the time period of microCT investigation, the soil of saplings was fully saturated with water and $\Psi_{stem}$ was measured periodically; for some saplings, the entire shoot was coated with petroleum jelly and covered with a sealed plastic bag containing a wet paper towel to test if minimizing transpiration affects tissue-specific refilling dynamics. For visualization of stem tissue, the potted sapling was placed in an aluminum cage, and the same stem portion located 2 to 3 cm above the soil was scanned repeatedly over a period of 24 h. Some saplings were transported back to the greenhouse and maintained under well-watered conditions for an additional 3 weeks before the stem portion was subjected to a rescan.

Excised stem samples were prepared within 5 to 8 h following branch harvest and were either rehydrated by supplying water to cut ends or sealed entirely. For both types of experiments, excised stem samples containing no leaves were prepared as follows. $\Psi_{stem}$ was measured on a bagged leaf of the branch that was located less than 2 cm away from the stem portion of interest. Immediately after, the branch was submerged in water, and a stem portion of 5 to 10 cm in length was cut under water with pruning shears. (1) For rehydrated excised stems, stem ends were recut using a fresh razor blade to remove air trapped at distal ends during the initial cut and, in turn, ensure maximal connectivity to externally supplied water. Following the procedure by Knipfer et al. (2016), the trimmed stem (length, 3–8 cm) was connected to a 2-cm piece of PVC tubing on the top end and to a 2-cm piece of PVC tubing attached to a valve (i.e. open position) on the bottom end. The tubing was sealed with the stem using high-vacuum grease (976V; Dow Corning). The PVC tubing was entirely filled with water, and the valve at the bottom end was closed. The stem with the attached tubing was removed from the water bath, and its entire surface was covered with vacuum grease to prevent surface evaporation. (2) For excised stems that were not supplied with water, stems were excised under water as described above and removed from the water bath, and the entire stem surface, including the cut stem ends, was coated with vacuum grease and wrapped with Parafilm to prevent evaporation. Following sample preparation, excised stems were placed in a sample holder, and the same stem portion about midway along the sample was scanned repeatedly over time.

Stems were scanned in a 21-keV synchrotron x-ray beam using a continuous tomography setting yielding 1,025 2D longitudinal images (resolution of 3.22 $\mu$m $pixel^{-1}$) that were captured on a CMOS camera (PCO.edge; PCO) at 350-ms exposure time. Acquired raw images were reconstructed into transverse images using a custom software plugin for Fiji image-processing software (www.fiji.sc; ImageJ) that used Octopus software (version 8.3; National Institutes for Nuclear Science, Ghent University) in the background (Knipfer et al., 2016). Longitudinal images were generated using the slice tool in the software AVIZO (version 6.2; Visualization Sciences Group/FEI).

The cross-sectional area of air-filled fibers, pith tissue, and vessels was quantified from binary images as generated from representative transverse microCT images using a semiautomated routine in Fiji software: for a time series of microCT images, the contrast and brightness were adjusted so that air-filled tissue was clearly visible at comparable intensity (Image-Adjust tool). Subsequently, the xylem including pith was extracted manually using the Image-Crop tool, and the Image-Threshold tool was used to label exclusively air-filled tissue; a noise filter was applied (Process-Noise-Despeckle tool) to remove black outlier pixels. Subsequently, labeled air-filled pith tissue was erased manually (Paint brush tool), and the remaining air-filled cross-sectional area of fibers and vessels ($A_{air\text{-}xylem}$) was measured (Analyze Particle tool). Following this step, labeled air-filled vessels were erased manually (Paint brush tool) from images, and the cross-sectional area of remaining air-filled fibers ($A_{air\text{-}fibers}$) was measured (Analyze Particle tool); the air-filled cross-sectional area of vessels ($A_{air\text{-}vessels}$) was determined by $A_{air\text{-}xylem} - A_{air\text{-}fibers}$. By using the original binary image again, $A_{air\text{-}xylem}$ was erased and the remaining cross-sectional area of air-filled pith ($A_{air\text{-}pith}$) was measured (Analyze Particle tool). The percentage changes of air-filled tissue was determined by $(A_{air\text{-}x\ (Scan2,3,\ldots,\ n)}/A_{air\text{-}x\ (Scan1)}) \times 100\%$ (where subscript x = fibers, pith tissue, or vessels). Based on these data, the rate of percentage reduction in $A_{air\text{-}fibers}$, $A_{air\text{-}pith}$, and $A_{air\text{-}vessels}$ over time was estimated using nonlinear regression analyses. In addition, contact angles of liquid/air menisci within the lumen of air-filled tissues were measured on longitudinal microCT images using the Angle tool in Fiji image-processing software (www.fiji.sc; ImageJ).

For 3D visualization, stems were imaged at higher resolution (1.27 $\mu$m $pixel^{-1}$). The stack of microCT images was uploaded into Fiji image-processing software (www.fiji.sc; ImageJ), and a semiautomated routine was used to segment air-filled portions of each tissue type: pith tissue was separated manually from xylem using the Polygon tool, and both images stacks were saved separately. The Image-Threshold tool was used to label air-filled fibers and vessels in one image stack and air-filled pith in the other image stack. For the binary image stack of air-filled fibers and vessels, the size criterion feature as part of the Analyze Particle tool was used to separate both air-filled tissue types, and image stacks were saved separately. Image stacks were inverted using Fiji software, uploaded into AVIZO software, and air-filled fibers, pith tissue, and vessels were visualized in 3D using the Volume Rendering tool.

Stem anatomy and tissue connectivity were studied on dry stem samples scanned at very high resolution (0.96 $\mu$m $pixel^{-1}$). For imaging, stem samples (around 3 cm in length) were prepared from branches harvested in the Arboretum at the University of California, Davis, and dehydrated slowly at around 30°C for 5 d prior to scanning. Tissue dimensions were determined from

microCT images using the Line and Polygon tools in Fiji image-processing software (www.fiji.sc; ImageJ).

## ESEM Imaging

ESEM experiments were performed to validate anatomical observations from microCT images. Stem samples (around 5 cm in length) were excised from branches collected at the University of California, Davis, Arboretum, placed in a plastic bag containing a wet paper towel, sent overnight to the ESEM facility at Yale University, stored at 4°C, and imaged less than 48 h after harvest. Samples were dissected with a razor blade to expose the xylem, and fresh tissue fragments of approximately 2 $mm^2$ were placed on a Peltier-cooled stage and maintained at 0.5°C during ESEM imaging. Samples were observed at 10 kV with a FEI/Philips Field Emission XL-30 ESEM device under true environmental mode. Water vapor was injected into the sample chamber at 4 Torr water vapor pressure, thereby establishing 95% relative humidity to prevent desiccation. With this sample preparation, no sputter coating was required.

## FDA-PI Viability Staining

Stem tissue viability was analyzed using a fluorescence-based staining assay (Krasnow et al., 2008; Knipfer et al., 2016). For analysis, two fluorescent dyes (FDA and PI) were used simultaneously that allow a two-color discrimination between living and dead tissue compartments (FDA can permeate through the intact cell membrane, and nonfluorescence FDA is converted into the green fluorescence metabolite fluorescein if cells are living and the esterase enzyme is active; PI cannot permeate through the intact cell membrane and stains the cell wall or the cell nuclei if the membrane is disrupted/leaky). The FDA-PI staining solution was prepared by adding 8 $\mu$L of FDA and 50 $\mu$L of PI to 5 mL of water. For analysis, stem samples were obtained from branches harvested at the Arboretum, University of California, Davis. Transverse stem sections were cut free handed using a fresh razor blade and were immediately submerged in the staining solution for 30 min and incubated in the dark at ~23°C. Subsequently, samples were mounted on a glass slide and observed under fluorescent light (excitation filters, 490 and 575 nm; dichromatic mirror, 505 nm; barrier filters, 525 and 625 nm) using a Leica DM4000 B LED microscope equipped with a Leica DFC7000 T 2.8 MP camera. Images were captured in less than 4 h following sample preparation.

## Supplemental Data

The following supplemental materials are available.

**Supplemental Figure S1.** Visualization of fiber refilling in an excised stem during rehydration for fibers that were located either close to or farther away from pith.

**Supplemental Table S1.** Summary of cross-sectional areas and $\Psi_{stem}$ of samples used in microCT experiments.

## ACKNOWLEDGMENTS

We thank D. Parkinson and A. MacDowell for assistance at the Lawrence Berkeley National Laboratory Advanced Light Source Beamline 8.3.2 microtomography facility.

Received August 11, 2017; accepted October 14, 2017; published October 17, 2017.

## LITERATURE CITED

**Beers EP** (1997) Programmed cell death during plant growth and development. Cell Death Differ **4:** 649–661

**Borchert R, Pockman WT** (2005) Water storage capacitance and xylem tension in isolated branches of temperate and tropical trees. Tree Physiol **25:** 457–466

**Brodersen CR, McElrone AJ** (2013) Maintenance of xylem network transport capacity: a review of embolism repair in vascular plants. Front Plant Sci **4:** 108

**Brodersen CR, McElrone AJ, Choat B, Matthews MA, Shackel KA** (2010) The dynamics of embolism repair in xylem: in vivo visualizations using high-resolution computed tomography. Plant Physiol **154:** 1088–1095

**Cai J, Li S, Zhang H, Zhang S, Tyree MT** (2014) Recalcitrant vulnerability curves: methods of analysis and the concept of fibre bridges for enhanced cavitation resistance. Plant Cell Environ **37:** 35–44

**Cermák J, Kucera J, Bauerle WL, Phillips N, Hinckley TM** (2007) Tree water storage and its diurnal dynamics related to sap flow and changes in stem volume in old-growth Douglas-fir trees. Tree Physiol **27:** 181–198

**Charrier G, Torres-Ruiz JM, Badel E, Burlett R, Choat B, Cochard H, Delmas CE, Domec JC, Jansen S, King A, et al** (2016) Evidence for hydraulic vulnerability segmentation and lack of xylem refilling under tension. Plant Physiol **172:** 1657–1668

**Choat B, Brodersen CR, McElrone AJ** (2015) Synchrotron x-ray microtomography of xylem embolism in *Sequoia sempervirens* saplings during cycles of drought and recovery. New Phytol **205:** 1095–1105

**Cochard H, Badel E, Herbette S, Delzon S, Choat B, Jansen S** (2013) Methods for measuring plant vulnerability to cavitation: a critical review. J Exp Bot **64:** 4779–4791

**Cochard H, Delzon S** (2013) Hydraulic failure and repair are not routine in trees. Ann For Sci **70:** 659–661

**De Schepper V, van Dusschoten D, Copini P, Jahnke S, Steppe K** (2012) MRI links stem water content to stem diameter variations in transpiring trees. J Exp Bot **63:** 2645–2653

**Esau K** (1953) Plant Anatomy. John Wiley and Sons, New York

**Goldstein G, Andrade JL, Meinzer FC, Holbrook NM, Cavelier J, Jackson P, Celis A** (1998) Stem water storage and diurnal patterns of water use in tropical forest canopy trees. Plant Cell Environ **21:** 397–406

**Hacke UG, Sperry JS** (2003) Limits to xylem refilling under negative pressure in *Laurus nobilis* and *Acer negundo*. Plant Cell Environ **26:** 303–311

**Hao GY, Wheeler JK, Holbrook NM, Goldstein G** (2013) Investigating xylem embolism formation, refilling and water storage in tree trunks using frequency domain reflectometry. J Exp Bot **64:** 2321–2332

**Holbrook NM** (1995) Stem water storage. *In* BL Gartner, ed, Plant Stem: Physiology and Functional Morphology. Academic Press, San Diego, pp 151–174

**Holbrook NM, Sinclair TR** (1992) Water balance in the arborescent palm, *Sabal palmetto*. II. Transpiration and stem water storage. Plant Cell Environ **15:** 401–409

**James SA, Meinzer FC, Goldstein G, Woodruff D, Jones T, Restom T, Mejia M, Clearwater M, Campanello P** (2003) Axial and radial water transport and internal water storage in tropical forest canopy trees. Oecologia **134:** 37–45

**Jupa R, Plavcová L, Gloser V, Jansen S** (2016) Linking xylem water storage with anatomical parameters in five temperate tree species. Tree Physiol **36:** 756–769

**Knipfer T, Brodersen CR, Zedan A, Kluepfel DA, McElrone AJ** (2015a) Patterns of drought-induced embolism formation and spread in living walnut saplings visualized using x-ray microtomography. Tree Physiol **35:** 744–755

**Knipfer T, Cuneo IF, Brodersen CR, McElrone AJ** (2016) In situ visualization of the dynamics in xylem embolism formation and removal in the absence of root pressure: a study on excised grapevine stems. Plant Physiol **171:** 1024–1036

**Knipfer T, Eustis A, Brodersen C, Walker AM, McElrone AJ** (2015b) Grapevine species from varied native habitats exhibit differences in embolism formation/repair associated with leaf gas exchange and root pressure. Plant Cell Environ **38:** 1503–1513

**Krasnow M, Matthews M, Shackel K** (2008) Evidence for substantial maintenance of membrane integrity and cell viability in normally developing grape (*Vitis vinifera* L.) berries throughout development. J Exp Bot **59:** 849–859

**LoGullo MA, Salleo S** (1988) Different strategies of drought resistance in three Mediterranean sclerophyllous trees growing in the same environmental conditions. New Phytol **108:** 267–276

**Meinzer FC, Johnson DM, Lachenbruch B, McCulloh KA, Woodruff DR** (2009) Xylem hydraulic safety margins in woody plants: coordination of stomatal control of xylem tension with hydraulic capacitance. Funct Ecol **23:** 922–930

**Nardini A, Lo Gullo MA, Tracanelli S** (1996) Water relations of six sclerophylls growing near Trieste (northeastern Italy): has scelrophylly a univocal functional significance? Giornale Botanica Italiano **130:** 811–828

**Nardini A, Savi T, Losso A, Petit G, Pacilè S, Tromba G, Mayr S, Trifilò P, Lo Gullo MA, Salleo S** (2017) X-ray microtomography observations of xylem embolism in stems of Laurus nobilis are consistent with hydraulic

measurements of percentage loss of conductance. New Phytol **213:** 1068–1075

**Oliva Carrasco L, Bucci SJ, Di Francescantonio D, Lezcano OA, Campanello PI, Scholz FG, Rodríguez S, Madanes N, Cristiano PM, Hao GY, et al** (2015) Water storage dynamics in the main stem of subtropical tree species differing in wood density, growth rate and life history traits. Tree Physiol **35:** 354–365

**Plavcová L, Jansen S** (2015) The role of xylem parenchyma in the storage and utilization of nonstructural carbohydrates. *In* U Hacke, ed, Functional and Ecological Xylem Anatomy. Springer International Publishing, Switzerland

**Pratt RB, Jacobsen AL** (2017) Conflicting demands on angiosperm xylem: tradeoffs among storage, transport and biomechanics. Plant Cell Environ **40:** 897–913

**Rhizopoulou S, Mitrakos K** (1990) Water relations of evergreen sclerophylls. I. Seasonal changes in the water relations of eleven species from the same environment. Ann Bot (Lond) **65:** 171–178

**Salleo S, Lo Gullo MA, De Paoli D, Zippo M** (1996) Xylem recovery from cavitation-induced embolism in young plants of *Laurus nobilis*: a possible mechanism. New Phytol **132:** 47–56

**Schweingruber FH, Boerner A, Schulze ED** (2011) Atlas of Stem Anatomy in Herbs, Shrubs and Trees, **Vol 1**. Springer-Verlag, Heidelberg, Germany

**Siau JF** (1984) Transport Processes in Wood. Springer-Verlag, Berlin

**Suuronen JP, Peura M, Fagerstedt K, Serimaa R** (2013) Visualizing water-filled versus embolized status of xylem conduits by desktop x-ray microtomography. Plant Methods **9:** 11

**Trifilò P, Raimondo F, Lo Gullo MA, Barbera PM, Salleo S, Nardini A** (2014) Relax and refill: xylem rehydration prior to hydraulic measurements favours embolism repair in stems and generates artificially low PLC values. Plant Cell Environ **37:** 2491–2499

**Tyree MT, Salleo S, Nardini A, Mosca R, Lo Gullo MA, Mosca R** (1999) Refilling of embolized vessels in young stems of laurel: do we need a new paradigm? Plant Physiol **120:** 11–22

**Tyree MT, Sperry JS** (1989) Vulnerability of xylem to cavitation and embolism. Annu Rev Plant Physiol Plant Mol Biol **40:** 19–38

**Tyree MT, Yang S** (1990) Water-storage capacity of *Thuja*, *Tsuga* and *Acer* stems measured by dehydration isotherms: the contribution of capillary water and cavitation. Planta **182:** 420–426

**Verbeeck H, Steppe K, Nadezhdina N, Op de Beeck M, Deckmyn G, Meiresonne L, Lemeur R, Cermák J, Ceulemans R, Janssens IA** (2007) Stored water use and transpiration in Scots pine: a modeling analysis with ANAFORE. Tree Physiol **27:** 1671–1685

**Waring RH, Whitehead D, Jarvis PG** (1979) The contribution of stored water to transpiration in Scots pine. Plant Cell Environ **2:** 309–317